Microenvironment and Immunology

Cancer
Research

B7-H1 Overexpression Regulates Epithelial–Mesenchymal Transition and Accelerates Carcinogenesis in Skin

Yujia Cao[1], Lu Zhang[1], Yosuke Kamimura[1], Patcharee Ritprajak[1], Masaaki Hashiguchi[1], Sachiko Hirose[2], and Miyuki Azuma[1]

Abstract

B7-H1 (CD274) is a T-cell coinhibitory molecule that is also often induced on human carcinoma cells, where its expression has been implicated in immune escape. Under inflammatory conditions, B7-H1 is also inducible in normal epithelial cells but little is known about its involvement in conversion of normal cells to tumor cells. Here, we show that skin-specific expression of B7-H1 accelerates inflammatory carcinogenesis in a methylcholantrene (MCA)-induced model of squamous cell carcinoma (SCC). Inflammatory responses induced by MCA or phorbol ester TPA were clearly inhibited in *B7-H1* transgenic mice (*B7-H1*tg mice). Antibody-mediated blockade of either B7-H1 or the related molecule PD-1 revealed that their ability to limit inflammation relied on ligand interactions made by B7-H1 or PD-1. Skin keratinocytes derived from B7-H1tg mice exhibited constitutive reduction of *E-cadherin*, and SCC induced in *B7-H1*tg mice also showed loss of *E-cadherin* along with elevated expression of the transcription factors *Slug* and *Twist* that drive epithelial–mesenchymal transition (EMT). Our results indicate that upregulation of B7-H1 in skin epithelial cells promotes EMT and accelerates carcinogenesis, revealing insights into the significance of B7-H1 overexpression on solid tumor cells and hinting at a close relationship between EMT and immune escape signaling pathways in cancer. *Cancer Res; 71(4); 1235–43. ©2010 AACR.*

Introduction

B7-H1 (CD274) is one of the ligands for the coinhibitory receptor PD-1 (CD279), and the B7-H1:PD-1 pathway is involved in the induction and maintenance of peripheral tolerance (1, 2). B7-H1 is widely distributed on leukocytes and nonhematopoietic cells in lymphoid and nonlymphoid tissues. Nonlymphoid tissue-associated B7-H1 is found on pancreatic islets (3), keratinocytes (KCs; ref. 4), smooth muscle cells (5), and placenta (6) at inflammatory disease sites. IFN-γ is a key cytokine in the induction of B7-H1. In addition to the expression of B7-H1 in normal tissue cells, constitutive expression of B7-H1 is found on various human cancers, including squamous cell carcinomas (SCCs) of the lung, esophagus, and head and neck; other types of carcinomas of the colon, ovaries, bladder, and breast; melanoma; and glioma (1, 7–17). Tumor-

associated B7-H1 is closely correlated with poor prognosis and/or higher malignancy grade. In mouse tumor transplants, B7-H1-transduced tumors show more aggressive tumor growth and poor survival rates (7, 9, 12). Ligation of PD-1 by tumor-associated B7-H1 induces apoptosis or downregulation of effector CTL, resulting in an escape from T-cell-mediated immune surveillance. Blockade of the B7-H1:PD-1 pathway efficiently reduces tumor growth and improves survival (7, 9, 12, 18, 19). Thus, tumor-associated B7-H1 apparently dampens host antitumor immune responses.

B7-H1 expression in breast cancer is strongly associated with proliferative Ki-67 expression and cell cycle progression that is independent of host PD-1 (16). In human glioma, cell surface B7-H1 is posttranscriptionally controlled and closely correlated with loss of "phosphatase and tensin homolog on chromosome ten" (PTEN), a tumor suppressor gene (20). KC-specific *Pten* deficiency resulted in epidermal hyperplasia and accelerated tumor formation, suggesting that PTEN may be an important regulator of carcinogenesis in the skin (21).

We recently generated B7-H1 transgenic mice under the control of human keratin 14 promoter (*B7-H1*tg) in which epidermal KCs overexpressed B7-H1 (22). No obvious abnormality was seen in the skin or hair of *B7-H1*tg mice, even in aged mice. KC-associated B7-H1 directly regulated effector CD8^{+} T-cell function at the cutaneous inflammatory sites of contact hypersensitivity. Although overexpression of B7-H1 on skin tumors has been reported, little is known about the role of B7-H1 in skin cancer formation. Recently, intradermal, but not subcutaneous, injection of 3-methylcholanthrene (MCA) was shown to preferentially induce SCCs rather than sarcomas (23). Here, we used this method to examine the frequency of

Authors' Affiliation: [1]Department of Molecular Immunology, Tokyo Medical and Dental University; and [2]Department of Pathology, Juntendo University School of Medicine, Tokyo, Japan.

Current address for P. Ritprajak, Cutaneous Biology Research Center, Massachusetts General Hospital and Harvard Medical School, Boston, MA 02114.

Current address for M. Hashiguchi, Department of Immunology, Dokkyo Medical University School of Medicine, Tochigi 321-0293, Japan.

Corresponding Author: Miyuki Azuma, Department of Molecular Immunology, Tokyo Medical and Dental University, 1-5-45 Yushima, Bunkyo-ku, Tokyo 113-8549, Japan. Phone and Fax: 03-5803-5935; E-mail: miyuki.mim@tmd.ac.jp.

AACR American Association for Cancer Research 1235

tumor formation in *B7-H1*tg mice and the phenotypic changes in KCs and SCCs.

Materials and Methods

Mice

B7-H1 transgenic mice under the control of the human *keratin 14* (K14) promoter (C57BL/6 *K14-B7-H1*tg; ref. 22) were backcrossed with BALB/c mice. Transgene-positive and transgene -negative mice were used as *B7-H1*$^{+/-}$ tg (*B7-H1*tg/hetero) and littermate (Lm) control mice, respectively. *B7-H1*tg/hetero female and male mice were bred and *B7-H1*$^{+/+}$ tg (*B7-H1*tg/homo) mice were obtained. BALB/c mice were purchased from Japan SLC (Shizuoka) and used as wild-type (wt) control mice for *B7-H1*tg/homo. *PD-1*-deficient mice with a BALB/c background (24) were kindly provided by Dr. Tasuku Honjo through RIKEN RBC and were maintained in our facility. All procedures were reviewed and approved by the Animal Care and Use Committee of Tokyo Medical and Dental University.

Induction of skin tumors

Skin tumors were induced as described by Wakita et al. (23) with minor modification. Mice were injected intradermally on the shaved right abdominal skin with 50 µL olive oil (Wako) containing 500 µg of MCA (Sigma-Aldrich) and monitored every week for the development of tumors. Skin tissues at the MCA injection sites were surgically removed at 3 and 7 days or at 7 weeks after MCA injection. Histological examination was performed. In separate experiments, the survival rate was monitored until 28 weeks.

TPA-induced skin inflammation

To induce skin inflammation, 12-*O*-tetradecanoylphorbol 13-acetate (TPA, 10 µg/200 µL in acetone; Alexis) was painted onto the shaved abdominal skin once or twice. For mAb blocking experiments, each group of mice received intraperitoneal (i.p.) injections of either control IgG (Cappel), anti-PD-1 (RMP1–14; ref. 25), or anti-*B7-H1* (MIH5) mAb (200 µg/ mouse; ref. 12) at days −1, 0, and 1 for 3 times. The painted sites of skin tissues were removed at 48 hours after the last painting.

Separation of epidermal sheets and isolation of epidermal cells

Dorsal halves of ear skin from intact or TPA-painted mice were incubated in 0.25% trypsin in PBS at 37°C for 45 minutes. The epidermal sheets were separated from the dorsal ear halves and used for the isolation of total RNA. For isolate single-cell suspensions of epidermal cells, the epidermal sheets were minced mechanically and filtered through nylon mesh. Single-cell suspensions of epidermal cells contained approximately 1% CD45$^+$CD49f$^-$ lymphocytes and 99% CD45$^-$CD49f$^+$ KCs, as assessed by flow cytometry.

Histology and immunohistochemistry

Paraffin-embedded tissue sections were stained with hematoxylin and eosin (H&E). Histology was assessed by 2 independent investigators. Cryostat sections were stained with anti-B7-H1 (MIH5) mAb, and enzymatic immunohistochemistry was performed as described previously (26).

Quantitative real-time RT-PCR

Total RNA was extracted from epidermal sheets or SCC tumor mass using Isogen (Nippongene). First-strand cDNA was synthesized using oligo (dT) primers and Superscript III reverse transcriptase (Invitrogen). Real-time PCR was performed using a LightCycler instrument with a DNA Master SYBR Green I kit (Roche Diagnostics). Primer sequences are listed in the Supplementary Table S1. Data are presented as the relative expression against β-actin (*Actb*).

Culture of primary established tumor cells

Tumor specimens generated from MCA-injected *B7-H1*tg mice were mechanically minced into small tissue fragments. The fragments were placed onto culture plates and cultured with DMEM supplemented with 10% FBS and gentamicin for 10–14 days. When a large enough number of tumor cells was grown from the fragments, the cells were detached by trypsinazation and reseeded onto fresh culture plates. Experiments were performed using the cells at passages 3 to 6. The type of SCC was confirmed by histological examination. Two primary cultured SCC cells (*B7-H1*tg/SCC1 and *B7-H1*tg/SCC2) were used in this study.

Tumor inoculation and evaluation of tumor growth

Colon26 (a BALB/c-originated colon adencarcinoma cell line) was kindly obtained from Cell Resource Center for Biomedical Research, Institute of Development, Aging and Center Tohoku University. Cells were cultured, freeze-stocked, and used in accordance with the United Kingdom Coordinating Committee on Cancer Research (UKCCCR) guidelines. Colon26 (5 × 10^5 cells and primary cultured SCC cells originating from *B7-H1*tg mice (*B7-H1*tg/SCC1 and *B7-H1*tg/SCC2, 5 × 10^4 cells) were injected intradermally into the shaved right flank of wt, *B7-H1*tg, or *PD-1*$^{-/-}$ BALB/c mice. In experiments to determine the involvement of B7-H1, 200 µg each of control IgG or ant-B7-H1 (MIH5) mAb were injected i.p. every other day after tumor inoculation. Tumor volumes were evaluated as described previously (27).

Statistics

Statistical analyses were performed using the Mann–Whitney *U*-test or Fisher's exact test. Values of $P < 0.05$ were considered significant.

Results

*B7-H1*tg mice overexpress B7-H1 on epidermal KCs

To confirm the expression of B7-H1 in epidermal KCs, we examined B7-H1 mRNA and protein levels. Epidermal KCs in *B7-H1*tg hetero and homo mice expressed high levels of mRNA and cell surface B7-H1 (Fig. 1A and 1B). The levels of mRNA and cell surface B7-H1 in *B7-H1*tg/hetero mice were almost half those of *B7-H1*tg/homo mice. Specific overexpression in the epidermis was confirmed by immunohistochemistry (Fig. 1C).
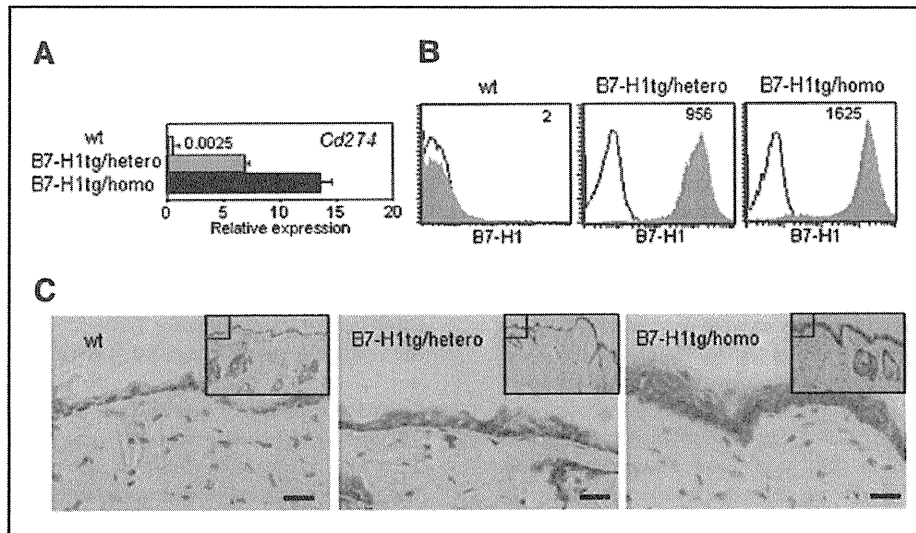
Figure 1. B7-H1tg mice overexpress B7-H1 on KCs. A, B7-H1 mRNA expression. Total RNA was extracted from epidermal sheets of ears from intact wt, B7-H1tg/hetero, and B7-H1tg/homo mice, and real-time PCR was performed. Values are means ± SD (n = 4). B, cell surface expression of B7-H1. Single-cell suspensions of epidermal sheets were stained with FITC-anti-CD49f (GoH3, BioLegend) and PE-anti-B7-H1 (MIH5, eBioscience), and APC-anti-CD45 (30-F11, eBioscience) or appropriate control mAbs. An electronic gate was placed on CD49f$^+$CD45$^-$ KCs and B7-H1 expression (filled histograms) is shown with control staining (plain line histograms). The values in the upper right are the mean fluorescence intensities. C, immunohistostaining for B7-H1. Cryostat sections of respective abdominal skin were immunostained with anti-B7-H1 (MIH5) mAb. Representative images are shown. Bars, 25 μm.

Earlier inflammatory responses are impaired in B7-H1tg mice

To investigate the role of B7-H1 in skin tumor formation, we used an intradermal injection of MCA to generate SCCs. No clear difference was observed between wt and B7-H1tg/homo mice before MCA injection (Fig. 2A). At 3 days after MCA injection, the epidermal thickness and number of epidermal layers were markedly increased, and these changes were more obvious in wt mice. Additionally, infiltration under the epidermal layers was more abundant in wt mice. At higher magnification, the alignment of basal cells in wt mice was well organized, whereas the basal cell alignment in the B7-H1tg mice was disturbed and more chromatin condensation was seen. At 7 days, the thickness of epidermis became comparable between wt and B7-H1tg mice. Careful observation revealed that the number of infiltrating cells in the supradermis (upper half) was clearly lower in the B7-H1tg mice, although infiltration in the deep dermis near the injected MCA/olive oil emulsion was abundant in both types of mice. The decreased inflammatory responses in B7-H1tg mice were confirmed by real-time PCR. The expression levels of IL-1α, IL-1β, IFN-γ, TNFα, and IL-6 were markedly impaired in the skin of B7-H1tg mice (Fig. 2B). In contrast, the expression of IL-10 (an antiinflammatory cytokine) was upregulated in B7-H1tg skin.

Topical painting of TPA also induced rapid basal KC proliferation and skin inflammation. Histology of TPA-painted skin showed proliferation of KCs and no clear difference in epidermal thickness or layer number between wt and B1-H1tg mice (Fig. 2C). Abundant cell infiltration was seen in the subepidermis of wt mice. Similar to the MCA-induced early inflammatory responses, cell infiltration in the B7-H1tg mice

was clearly impaired. To clarify the involvement of B7-H1 and PD-1 interactions in the impaired inflammatory responses, TPA-painted mice received i.p. injection with control IgG, anti-PD-1 mAb or anti-B7-H1 mAb for 3 days and then a histological analysis was conducted. Treatment with anti-PD-1 or anti-B7-H1 mAb, but not control IgG, dramatically enhanced the infiltration level in B7-H1tg mice (Fig. 2C), but the same treatment did not clearly affect wt mice (data not shown). These results suggest the involvement of the B7-H1:PD-1 pathway in the impaired inflammatory responses in B7-H1tg mice. To identify PD-1-expressing cells within the epidermis and dermis, we analyzed PD-1 expression by flow cytometry. A minor fraction of PD-1^{dim} positive cells (~5%) was found within CD45$^+$CD49f$^-$ epidermal lymphocytes. These cells expressed very low levels of CD3ε and lacked CD11c and TCRγδ expression (data not shown). No PD-1$^+$ cells were observed in the dermis fraction. Further studies are needed to clarify the target cells involved in the B7-H1:PD-1-mediated reduction of inflammatory responses.

Epidermal tumor formation is promoted in B7-H1tg mice

MCA-injected mice were monitored weekly for the development of primary tumors, and tumor masses were resected at 7 weeks for histological analysis. Representative images of well-differentiated SCC with cancer pearl (Fig. 3A, a), undifferentiated SCC with spindle phenotype (Fig. 3A, b), and basal cell carcinoma (BCC; Fig. 3A, c) are shown. In most SCCs, scattered small colonies were observed near the cyst wall (Fig. 3A, d), suggesting that the SCC cells were derived from the epithelium of cyst walls. Overall tumor incidence was approximately
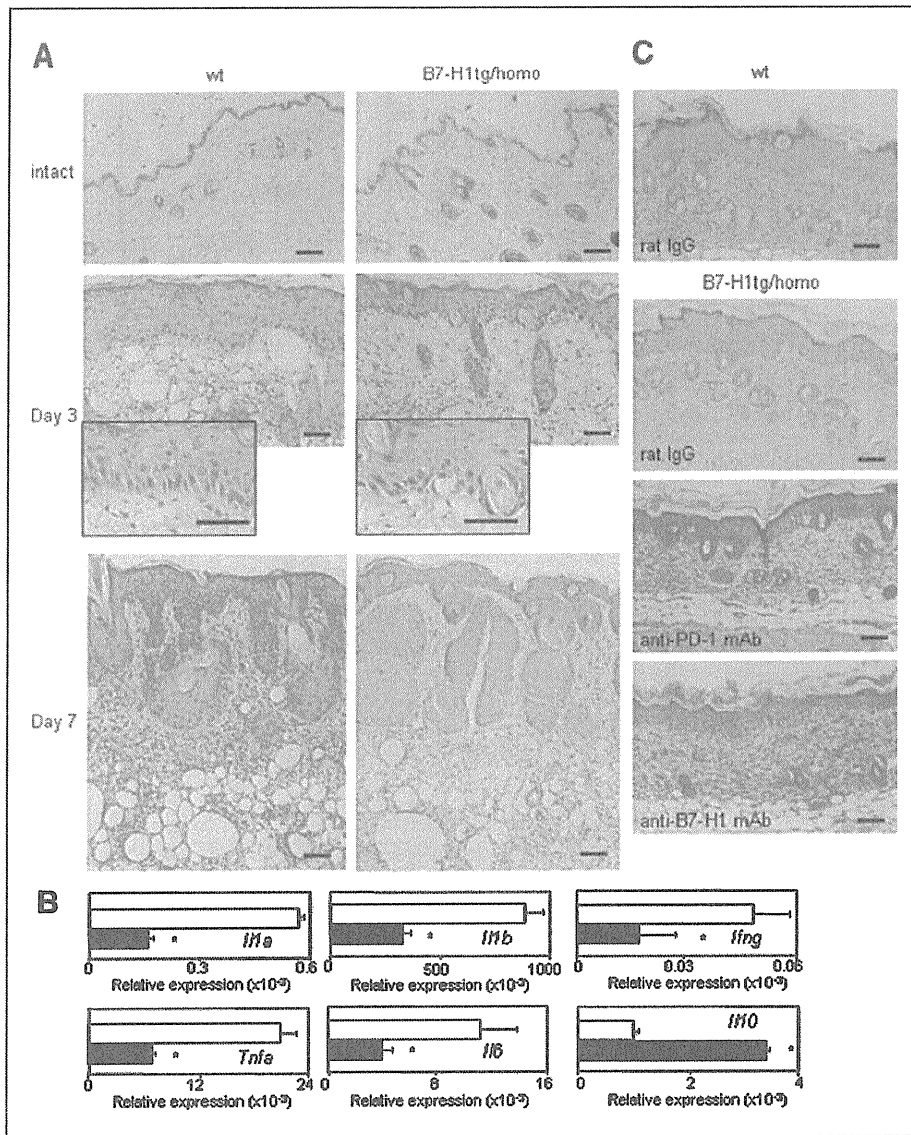
— 154 —

Figure 2. Skin inflammatory responses are suppressed in B7-H1tg mice. A, H&E staining of intact or MCA-injected skin tissues at days 3 and 7. Bars, 100 μm. B, mRNA was extracted from whole skin tissues of MCA-injected sites from wt (open columns) and B7-H1tg (closed columns) mice at day 7. Cytokine expression was analyzed by real-time PCR. Values are means ± SD (n = 3). Data are representative of 2 independent experiments. C, H&E staining of skin sections at 48 h after the last TPA painting and mAb treatment. Bars, 100 μm.

threefold higher in *B7-H1*tg/homo and twofold higher in *B7-H1*tg/hetero compared with Lm control (Table 1). The incidence of SSC was significantly higher in both *B7-H1*tg homo and hetero mice. The incidence of basal cell tumors (BCTs), including basal cell epitheliomas and BCCs, also was increased significantly in *B7-H1*tg/homo mice. When we monitored the survival rates until 28 weeks after MCA injection, the final survival rate of *B7-H1*tg/homo mice was 20%, which was threefold less than that of wt mice (Fig. 3B). All surviving mice were tumor-free. These results demonstrate that KC-derived tumor formation was promoted in *B7-H1*tg mice.

Next, B7-H1 status was compared between wt and *B7-H1*tg mice. Both KCs and SCCs from wt mice expressed very low levels of B7-H1 transcripts. However, both KCs and SCCs from *B7-H1*tg mice showed persistently much higher levels of B7-H1 (Fig. 3C). Immunohistochemistry of B7-H1 in the *B7-H1*tg-SCC

sections showed extremely strong B7-H1 expression in the epidermis, hair follicles, and SCC tumor sites (Fig. 3D). These results indicate that *B7-H1*tg-SCCs consistently possessed similar feature in terms of B7-H1 status, suggesting the conversion of KCs to SCCs.

E-cadherin is downregulated in B7-H1–overexpressing KCs

To address why B7-H1-overexpression in KCs induced higher tumor formation, we focused on molecules involved in the epithelial–mesenchymal transition (EMT; ref. 28, 29). Loss of E-cadherin and upregulation of N-cadherin have been closely correlated with migratory properties of epithelial cells to mesenchymal cells. Thus, transcripts for E-cadherin (*Cdh1*) and N-cadherin (*Cdh2*) in KCs and SCCs were compared between wt and *B7-H1*tg mice, using with K14 *(Krt14)* to
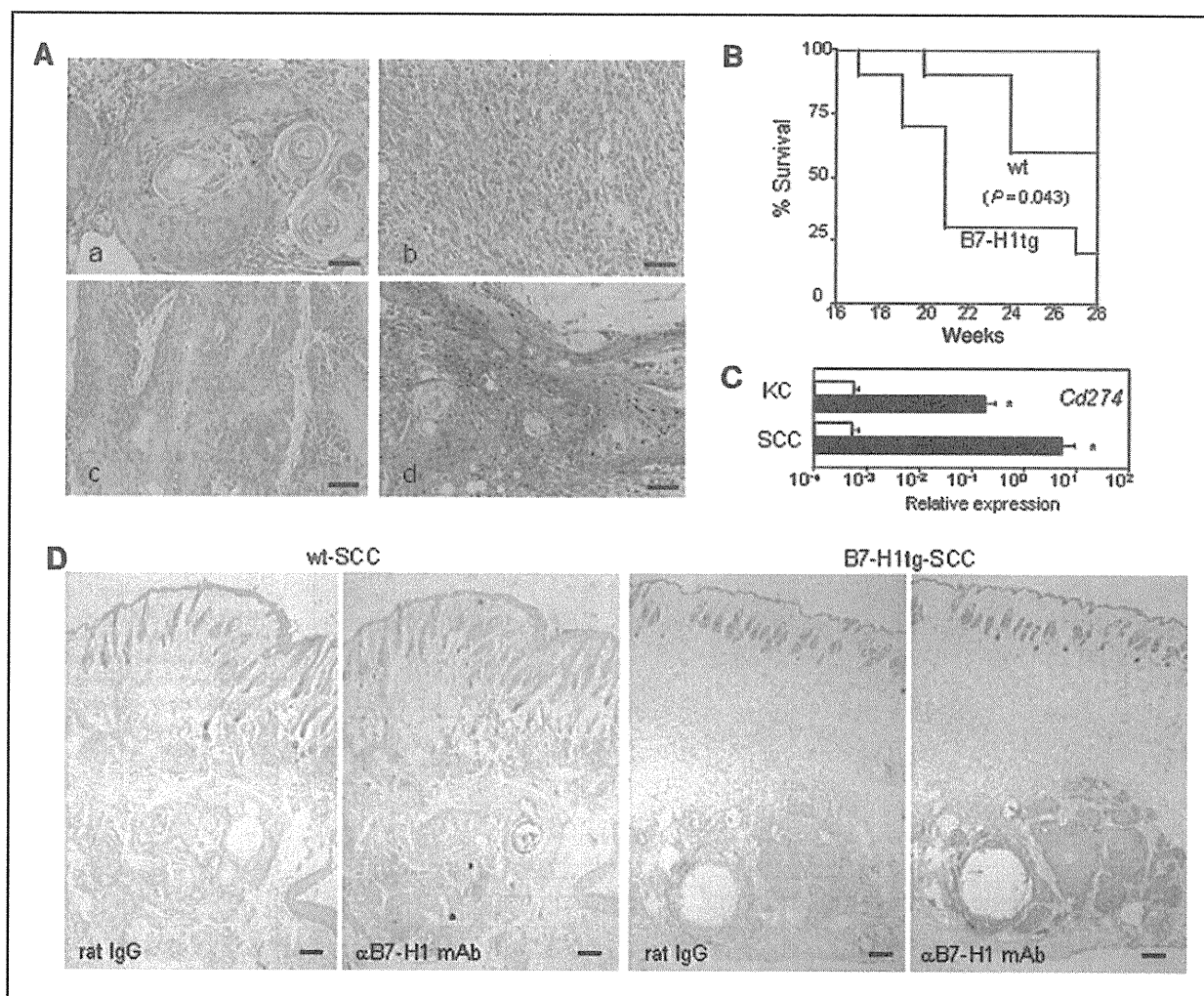
— 155 —

Figure 3. MCA-induced skin tumors. A, H&E staining of representative tumor tissue types 7 weeks after MCA injection. Representative images are shown of a well-differentiated SCC (a), undifferentiated SCC (b), basal cell carcinoma (BCC) (c), and scattered small colonies of SCCs near the cyst (d). Bars, 50 μm. B, survival curves after MCA injection. Data ($n = 10$) are representative of 2 independent experiments. C, real-time PCR for B7-H1. Intact epidermal sheets and SCCs from wt (open columns) and B7-H1tg (closed columns) mice were analyzed. Values are means ± SD ($n = 3$). D, immunohistostaining of B7-H1. Frozen sections of SCC tumor sites at 7 weeks after MCA injection were stained with either control rat IgG or anti-B7-H1 mAb. Bars, 250 μm.

assess the quantity of epidermal cells. KCs from *B7-H1*tg mice showed significantly lower *Cdh1* expression, despite comparable levels of *Krt14* (Fig. 4A). After the conversion to SCCs, *Cdh1* levels in the SCCs were markedly decreased in both types of mice, but were consistently lower in *B7-H1*tg. In contrast, *Cdh2* clearly increased after SCC conversion, with no apparent difference between wt and *B7-H1*tg mice. To directly confirm the preferential loss of E-cadherin in *B7-H1*tg-KCs, *Krt14* and *Cdh1* expression was examined 24 hours after topical TPA painting. TPA painting clearly enhanced the *Krt14* transcripts in KCs of both wt and *B7-H1*tg mice, suggesting comparable expansion of KCs; however, TPA stimulation further downregulated *Cdh1* in both wt and *B7-H1*tg.

Downregulation of E-cadherin has been shown to be controlled by transcription repressors, such as Snail and Slug (29,

30). Thus, we next examined Snail (*Snail*), Slug (*Snai2*), and Twist (*Twist*) transcription levels. Intact KCs did not show substantial levels of these transcripts, and no difference was observed between wt and *B7-H1*tg (Fig. 4B). After SCC conversion, levels of all 3 were dramatically increased, but the increased levels of *Snai2* and *Twist* were significantly higher in the *B7-H1*tg-SCCs. No clear difference was seen in *Snail* expression. These results suggest that the higher incidence of skin tumor formation in *B7-H1*tg mice may be related to a loss of E-cadherin and the preferential upregulation of Slug and Twist.

PD-1–mediated host immune responses are involved in the enhanced tumor formation

We next examined whether B7-H1- or PD-1-mediated antitumor host responses are involved in the accelerated SCC

— 156 —

Table 1 Tumor incidence 7 weeks after MCA injection

Group	(n)	Tumor Incidence (%)[a]			
		Total tumors	BCT	SCC	FS
wt control	42	19.0 (8)	2.4 (1)	14.3 (6)	2.4 (1)
B7-H1tg/homo	40	62.5[b] (25)	15.0[b] (6)	42.5 (17)	5.0 (2)
Lm control	32	43.7 (14)	9.4 (3)	31.2 (10)	3.1 (1)
B7-H1tg/hetero	35	68.8[b] (24)	11.4 (4)	57.1[b] (20)	0.0 (0)

[a]Skin tissues at the MCA-injected sites were removed after 7 weeks and histological examination was performed. Values are the data from 3 to 4 independent experiments. BCT, basal cell tumors including basal cell epithelioma and basal cell carcinoma; SCC, squamous cell carcinoma; FS, fibrosarcoma.
[b]Statistically different from each control group ($P < 0.05$).

formation. To address whether over-expressing B7-H1 on KCs affects antitumor immune responses against B7-H1[negative-low] tumors, Colon26 tumor cells, which expressed very low levels of B7-H1 (Fig. 5A), were inoculated into wt and *B7-H1*tg mice, and tumor growth was examined. No clear difference was observed between their growth curves (Fig. 5B). In addition, the analyses of regional lymph nodes 10 days after tumor inoculation showed no clear differences in the total cell number, the proportions of $CD3^+$, $CD4^+$, and $CD8^+$ T cells; or IFN-γ expression in $CD4^+$ and $CD8^+$ T cells (data not

shown). These results indicate that B7-H1 overexpression in KCs does not affect antitumor immune responses against the tumors that express endogenous low levels of B7-H1.

After the malignancy conversion from KCs, the growth of B7-H1-overexpressing tumor cells may be affected by antitumor immune responses. To investigate the involvement of PD-1 and/or B7-H1 in antitumor responses against B7-H1 overexpressing tumors, we compared tumor growth between wt and $PD-1^{-/-}$ mice inoculated with *B7-H1*tg-derived SCC cells, which expressed cell surface B7-H1 at
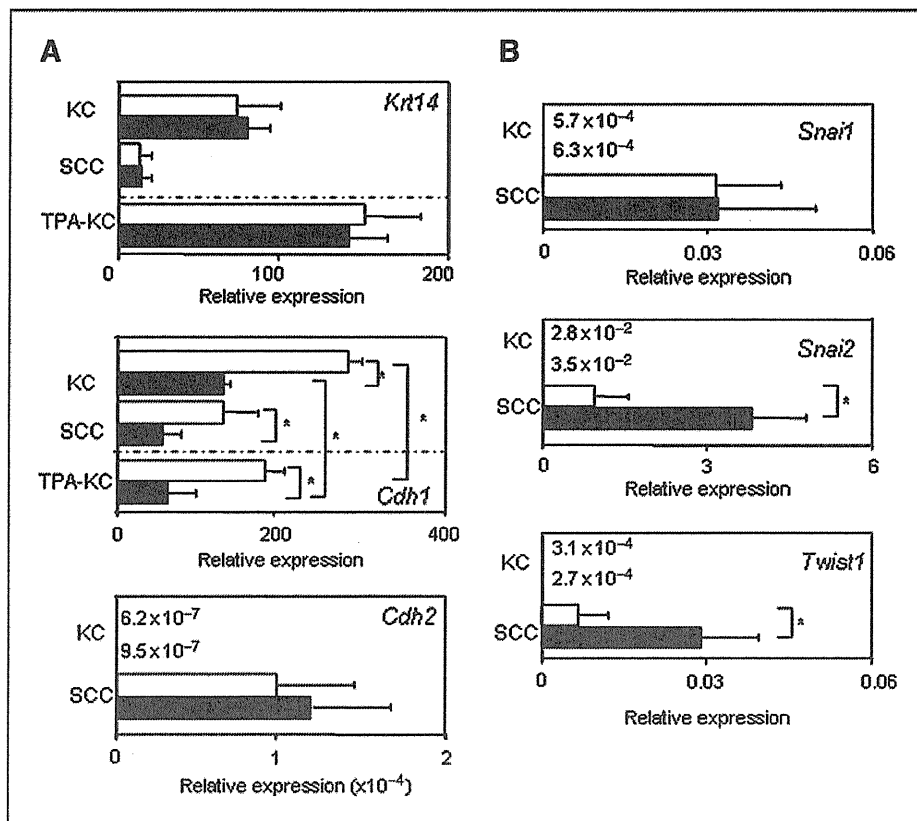

Figure 4. Transcripts of EMT-related molecules. A and B, total RNA was isolated from epidermal sheets of intact skin (KC), TPA-painted skin at 24 hours (TPA-KC), and SCC tumor mass (SCC) from wt (open columns) and B7-H1tg (closed columns) mice. The expression of the indicated genes was analyzed by real-time PCR. Values shown are means ± SD ($n = 5$–7). *, statistically significant ($P < 0.05$).

— 157 —

very high levels (Fig. 5A). To mimic early stage of tumors development, we intradermally inoculated 10-fold few tumor cells (5 × 10⁴ cells) than in the experiments using colon26. The wt mice permitted the growth of *B7-H1*tg-derived primary tumor cells, whereas *PD-1*-deficient mice completely rejected the tumor engraftment (Fig. 5C). Anti-B7-H1 mAb treatment in *PD-1*-deficient mice canceled the tumor rejection, and tumor growth was comparable to that in wt mice (Fig. 5D). These results suggest that PD-1-mediated host responses against B7-H1-overexpressing tumors are involved in accelerated tumor formation.

Discussion

We demonstrated for the first time that SCC formation was promoted in B7-H1-overexpressing skin. Our results indicate that downregulation of E-cadherin in *B7-H1*tg mice occurs prior to tumor development. Without stimulation, E-cadherin expression in intact KCs was constitutively downregulated in *B7-H1*tg mice (Fig. 4A). The disturbed alignment and atypical change of basal KCs observed in *B7-H1*tg mice at the earlier time point (Fig. 2A) suggest dysregulation of cell adhesion and rapid cancerous changes in basal KCs.

TGF-β1 and its related signaling have been shown to contribute greatly to the suppression of EMT or progression of tumor invasion and metastasis during skin carcinogenesis (31, 32). Although we compared *TGF-β1* expression in MCA-induced inflammatory skin (Supplementary Fig. S1), intact KCs and SCCs (Supplementary Fig. S2) between wt and *B7-H1*tg mice, no obvious difference was observed. *TGF-β1* expression was rather decreased both in the inflammatory skin and after SCC conversion. Thus, it is unlikely that the TGF-β pathway was involved in the increased carcinogenesis in *B7-H1*tg mice.

The inflammatory microenvironment promotes EMT-like changes in the skin and upregulation of Snail and Slug seems to occur as an upstream event prior to loss of E-cadherin (29, 30, 33). Our study revealed that inflammatory responses were markedly reduced in the skin of *B7-H1*tg mice in experiments with both MCA injection and TPA painting. Thus, we could not attribute the increased tumor formation in *B7-H1*tg mice to inflammation-induced tumor formation. Short-time TPA stimulation did not upregulate Snail, Slug, or Twist expression (data not shown). Preferential upregulation of Slug and Twist may occur in *B7-H1*tg during the tumor progression process after the loss of E-cadherin. Snail and Slug have been shown to contribute to cell survival and apoptosis resistance (34–36). In an ultraviolet radiation-induced murine SCC model, Snail and Slug upregulation was mediated by activation of the mitogen-activated protein kinase kinase (MAPK)/extracellular signal-regulated kinase (ERK) signaling cascade (36). Transcriptional repression of E-cadherin requires activation of MAPK/ERK signaling (37, 38). Presently, we cannot identify specific molecules involved in the B7-H1-mediated regulation of E-cadherin, Slug, and Twist expression. It is possible that overexpression of B7-H1 may transduce constitutive signals, resulting in activation of the MAPK/ERK signaling cascade. A common signaling
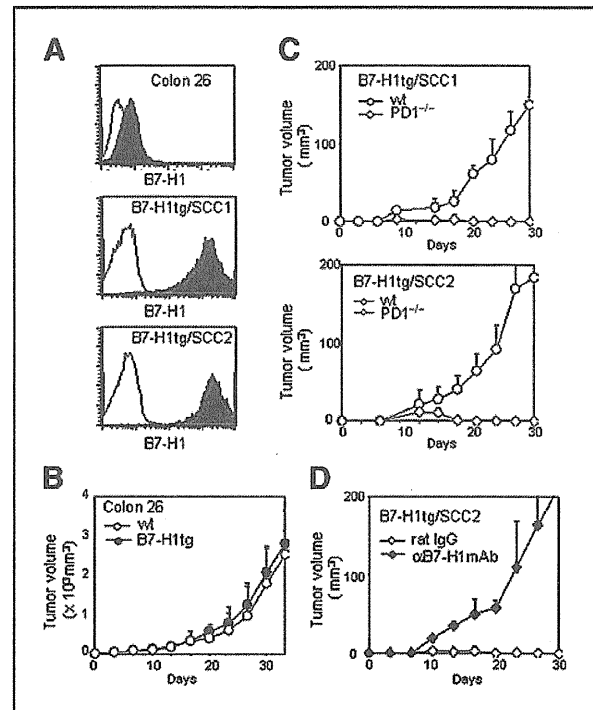

Figure 5. Involvement of the B7-H1:PD-1 pathway in B7-H1–negative or –overexpressing tumor growth. A, expression of B7-H1. Colon26, B7-H1tg/SCC1, and B7-H1tg/SCC2 cell lines were stained with PE-conjugated anti-B7-H1 mAb or control IgG and analyzed by flow cytometry. Data are shown as filled histograms with control staining as plain-line histograms. B–D, Colon26 (5 × 10⁵ cells), B7-H1tg/SCC1 or B7-H1tg/SCC2 (5 × 10⁴ cells) were intradermally injected into syngeneic BALB/c wt (open circles), B7-H1tg (closed circles), or PD-1⁻/⁻ (diamonds) mice and tumor volumes were monitored. In D, tumor-inoculated mice received an intraperitoneal injection of control rat IgG (open diamonds) or anti-B7-H1 mAb (closed diamonds) (200 μg/mouse) 3 times a week. The mean tumor volume ± SD was determined in each group of 5 mice.

cascade may regulate different target molecules that promote EMT during the development of tumors. We investigated whether persistent upregulation of endogenously induced B7-H1 by IFN-γ stimulation in murine SCC cell lines (NRS-1 and SCCVII) could induce downregulation of E-cadherin. The expression levels of E-cadherin were comparable before and after treatment for 2 weeks (data not shown). Cell surface expression on primary *B7-H1*tg/SCC cell cultures was approximately 50-fold higher than that of endogenously induced B7-H1 on SCC cell lines. Thus, the promoted carcinogenesis observed in our study may occur in only limited situations. Further studies are needed to address the signaling involved in B7-H1-mediated E-cadherin regulation.

Although the loss of *Pten*, a tumor suppressor gene, has been reported in B7-H1-overexpressing tumors (20), the B7-H1 transgene of B7-H1 did not alter *Pten* expression in *B7-H1*tg KCs and SCCs (Supplementary Fig. S2), Antiapoptotic reverse signaling of B7-H1 in cancer cells has been also reported (39). Therefore, we examined the effects of B7-H1-mediated reverse signaling by stimulation with immobilized PD-1Ig

— 158 —

or anti-B7-H1 mAb-conjugated polystyrene beads. No morphological and phenotypic changes and no anti-apoptotic effects were seen in the *B7-H1tg*/SCC cells. The mRNA expression for cell cycle related Cyclin D1 (*Ccnd1*) and antiapoptotic Bcl2 (*Bcl2*) was also comparable between wt and *B7-H1tg* SCCs (Supplementary Fig. S2). These results suggest that *B7-H1tg* SCCs do not possess obviously distinct features in cell cycle progression and antiapoptosis.

After the atypical change or malignancy conversion from normal KCs, PD-1-mediated regulation in antitumor immune responses may strongly contribute to the promotion of tumor growth because of the much higher expression of B7-H1. Indeed, our results suggest that tumor growth of *B7-H1tg*-derived SCC cells was completely dependent on the B7-H1-PD-1 pathway. Overexpression of B7-H1 in KCs may promote an early stage of carcinogenesis via intrinsic cell change; however, after this process, PD-1-mediated host immune responses greatly contribute the accelerated tumor formation.

The studies using human SCC specimens of the esophagus, skin, head and neck, and oral cavity demonstrated that the decreased E-cadherin expression was associated with increased invasiveness, lymph node metastasis, and/or poor survival (40–43). Immunohistological analyses in esophageal SCCs revealed that the elevated Slug or Twist expression was significantly correlated with reduced E-cadherin and showed poor clinical outcomes (44, 45). Another study also demonstrated that Twist expression in esophageal SCCs served as an independent prognostic factor for predicting distant metastasis and survival (46). B7-H1 expression has shown to be closely correlated with poor prognosis and/or higher malignancy grade in esophageal SCCs (11). Although no parallel study for B7-H1 expression and E-cadherin or EMT-inducing transcription factors has been reported, the above results suggest a close correlation between upregulation of B7-H1 expression and reduced E-cadherin and/or enhanced Slug and Twist transcription factors in human

SCCs. Further studies including *in situ* detection of EMT-related molecules and B7-H1 expression in the invasive front of human SCC samples are required.

In conclusion, the overexpression of B7-H1 accelerates skin tumor development, despite marked B7-H1-mediated reduction of skin inflammation. Our data show that B7-H1 serves a new role; the promotion of EMT via downregulation of E-cadherin and upregulation of Slug and Twist. Our results indicate that B7-H1 in KCs may function as an antiinflammatory molecule for short-term inflammation, but persistent overexpression of B7-H1 by continuous or repeated stimulation may cause intrinsic changes within the cell and promote carcinogenesis. Our study provides new insights into B7-H1 function in inflammation and cancer development.

Disclosure of Potential Conflicts of Interest

No potential conflicts of interest were disclosed.

References

1. Zou W, Chen L. Inhibitory B7-family molecules in the tumour microenvironment. Nat Rev Immunol 2008;8:467–77.
2. Keir ME, Butte MJ, Freeman GJ, Sharpe AH. PD-1 and its ligands in tolerance and immunity. Annu Rev Immunol 2008;26: 677–704.
3. Ansari MJ, Salama AD, Chitnis T, et al. The programmed death-1 (PD-1) pathway regulates autoimmune diabetes in nonobese diabetic (NOD) mice. J Exp Med 2003;198:63–9.
4. Youngnak-Piboonratanakit P, Tsushima F, Otsuki N, et al. The expression of B7-H1 on keratinocytes in chronic inflammatory mucocutaneous disease and its regulatory role. Immunol Lett 2004;94: 215–22.
5. Koga N, Suzuki J, Kosuge H, et al. Blockade of the interaction between PD-1 and PD-L1 accelerates graft arterial disease in cardiac allografts. Arterioscler Thromb Vasc Biol 2004;24:2057–62.
6. Guleria I, Khosroshahi A, Ansari MJ, et al. A critical role for the programmed death ligand 1 in fetomaternal tolerance. J Exp Med 2005;202:231–7.
7. Dong H, Strome SE, Salomao DR, et al. Tumor-associated B7-H1 promotes T-cell apoptosis: a potential mechanism of immune evasion. Nat Med 2002;8:793–800.
8. Wintterle S, Schreiner B, Mitsdoerffer M, et al. Expression of the B7-related molecule B7-H1 by glioma cells: a potential mechanism of immune paralysis. Cancer Res 2003;63:7462–7.

9. Strome SE, Dong H, Tamura H, et al. B7-H1 blockade augments adoptive T-cell immunotherapy for squamous cell carcinoma. Cancer Res 2003;63:6501–5.
10. Konishi J, Yamazaki K, Azuma M, Kinoshita I, Dosaka-Akita H, Nishimura M. B7-H1 expression on non-small cell lung cancer cells and its relationship with tumor-infiltrating lymphocytes and their PD-1 expression. Clin Cancer Res 2004;10:5094–100.
11. Ohigashi Y, Sho M, Yamada Y, et al. Clinical significance of programmed death-1 ligand-1 and programmed death-1 ligand-2 expression in human esophageal cancer. Clin Cancer Res 2005;11: 2947–53.
12. Tsushima F, Tanaka K, Otsuki N, et al. Predominant expression of B7-H1 and its immunoregulatory roles in oral squamous cell carcinoma. Oral Oncol 2006;42:268–74.
13. Thompson RH, Kwon ED. Significance of B7-H1 overexpression in kidney cancer. Clin Genitourin Cancer 2006;5:206–11.
14. Hamanishi J, Mandai M, Iwasaki M, et al. Programmed cell death 1 ligand 1 and tumor-infiltrating CD8+ T lymphocytes are prognostic factors of human ovarian cancer. Proc Natl Acad Sci USA 2007; 104:3360–5.
15. Nomi T, Sho M, Akahori T, et al. Clinical significance and therapeutic potential of the programmed death-1 ligand/programmed death-1 pathway in human pancreatic cancer. Clin Cancer Res 2007;13: 2151–7.

— 159 —

16. Ghebeh H, Tulbah A, Mohammed S, et al. Expression of B7-H1 in breast cancer patients is strongly associated with high proliferative Ki-67-expressing tumor cells. Int J Cancer 2007;121:751–8.

17. Yao Y, Tao R, Wang X, Wang Y, Mao Y, Zhou LF. B7-H1 is correlated with malignancy-grade gliomas but is not expressed exclusively on tumor stem-like cells. Neuro Oncol 2009;11:757–66.

18. Iwai Y, Terawaki S, Honjo T. PD-1 blockade inhibits hematogenous spread of poorly immunogenic tumor cells by enhanced recruitment of effector T cells. Int Immunol 2005;17:133–44.

19. Hirano F, Kaneko K, Tamura H, et al. Blockade of B7-H1 and PD-1 by monoclonal antibodies potentiates cancer therapeutic immunity. Cancer Res 2005;65:1089–96.

20. Parsa AT, Waldron JS, Panner A, et al. Loss of tumor suppressor PTEN function increases B7-H1 expression and immunoresistance in glioma. Nat Med 2007;13:84–8.

21. Suzuki A, Itami S, Ohishi M, et al. Keratinocyte-specific Pten deficiency results in epidermal hyperplasia, accelerated hair follicle morphogenesis and tumor formation. Cancer Res 2003;63:674–81.

22. Ritprajak P, Hashiguchi M, Tsushima F, Chalermsarp N, Azuma M. Keratinocyte-associated B7-H1 directly regulates cutaneous effector CD8+ T cell responses. J Immunol 2010;184:4918–25.

23. Wakita D, Chamoto K, Ohkuri T, et al. IFN-γ-dependent type 1 immunity is crucial for immunosurveillance against squamous cell carcinoma in a novel mouse carcinogenesis model. Carcinogenesis 2009;30:1408–15.

24. Nishimura H, Okazaki T, Tanaka Y, et al. Autoimmune dilated cardiomyopathy in PD-1 receptor-deficient mice. Science 2001;291:319–22.

25. Yamazaki T, Akiba H, Koyanagi A, Azuma M, Yagita H, Okumura K. Blockade of B7-H1 on macrophages suppresses CD4+ T cell proliferation by augmenting IFN-γ-induced nitric oxide production. J Immunol 2005;175:1586–92.

26. Chalermsarp N, Azuma M. Identification of three distinct subsets of migrating dendritic cells from oral mucosa within the regional lymph nodes. Immunology 2009;127:558–66.

27. Mogi S, Sakurai J, Kohsaka T, et al. Tumour rejection by gene transfer of 4-1BB ligand into a CD80+ murine squamous cell carcinoma and the requirements of co-stimulatory molecules on tumour and host cells. Immunology 2000;101:541–7.

28. Takeichi M. Morphogenetic roles of classic cadherins. Curr Opin Cell Biol 1995;7:619–27.

29. Cano A, Perez-Moreno MA, Rodrigo I, et al. The transcription factor snail controls epithelial-mesenchymal transitions by repressing E-cadherin expression. Nat Cell Biol 2000;2:76–83.

30. Bolos V, Peinado H, Perez-Moreno MA, Fraga MF, Esteller M, Cano A. The transcription factor Slug represses E-cadherin expression and induces epithelial to mesenchymal transitions: a comparison with Snail and E47 repressors. J Cell Sci 2003;116:499–511.

31. Han G, Lu SL, Li AG, et al. Distinct mechanisms of TGF-β1-mediated epithelial-to-mesenchymal transition and metastasis during skin carcinogenesis. J Clin Invest 2005;115:1714–23.

32. Hoot KE, Lighthall J, Han G, et al. Keratinocyte-specific Smad2 ablation results in increased epithelial-mesenchymal transition during skin cancer formation and progression. J Clin Invest 2008;118:2722–32.

33. St John MA, Dohadwala M, Luo J, et al. Proinflammatory mediators upregulate snail in head and neck squamous cell carcinoma. Clin Cancer Res 2009;15:6018–27.

34. Olmeda D, Montes A, Moreno-Bueno G, Flores JM, Portillo F, Cano A. Snail and Snai2 collaborate on tumor growth and metastasis properties of mouse skin carcinoma cell lines. Oncogene 2008;27:4690–701.

35. Newkirk KM, Parent AE, Fossey SL, et al. Snai2 expression enhances ultraviolet radiation-induced skin carcinogenesis. Am J Pathol 2007;171:1629–39.

36. Hudson LG, Choi C, Newkirk KM, et al. Ultraviolet radiation stimulates expression of Snail family transcription factors in keratinocytes. Mol Carcinog 2007;46:257–68.

37. Conacci-Sorrell M, Simcha I, Ben-Yedidia T, Blechman J, Savagner P, Ben-Ze'ev A. Autoregulation of E-cadherin expression by cadherin-cadherin interactions: the roles of beta-catenin signaling, Slug, and MAPK. J Cell Biol 2003;163:847–57.

38. Pece S, Gutkind JS. Signaling from E-cadherins to the MAPK pathway by the recruitment and activation of epidermal growth factor receptors upon cell-cell contact formation. J Biol Chem 2000;275:41227–33.

39. Azuma T, Yao S, Zhu G, Flies AS, Flies SJ, Chen L. B7-H1 is a ubiquitous antiapoptotic receptor on cancer cells. Blood 2008;111:3635–43.

40. Kaihara T, Kusaka T, Kawamata H, et al. Decreased expression of E-cadherin and Yamamoto-Kohama's mode of invasion highly correlates with lymph node metastasis in esophageal squamous cell carcinoma. Pathobiology 2001;69:172–8.

41. Papadavid E, Pignatelli M, Zakynthinos S, Krausz T, Chu AC. Abnormal immunoreactivity of the E-cadherin/catenin (α-, β-, and γ-) complex in premalignant and malignant non-melanocytic skin tumours. J Pathol 2002;196:154–62.

42. Eriksen JG, Steiniche T, Sogaard H, Overgaard J. Expression of integrins and E-cadherin in squamous cell carcinomas of the head and neck. APMIS 2004;112:560–8.

43. Pyo SW, Hashimoto M, Kim YS, et al. Expression of E-cadherin, P-cadherin and N-cadherin in oral squamous cell carcinoma: correlation with the clinicopathologic features and patient outcome. J Craniomaxillofac Surg 2007;35:1–9.

44. Uchikado Y, Natsugoe S, Okumura H, et al. Slug Expression in the E-cadherin preserved tumors is related to prognosis in patients with esophageal squamous cell carcinoma. Clin Cancer Res 2005;11:1174–80.

45. Sasaki K, Natsugoe S, Ishigami S, et al. Significance of Twist expression and its association with E-cadherin in esophageal squamous cell carcinoma. J Exp Clin Cancer Res 2009;28:158–66.

46. Xie F, Li K, Ouyang X. Twist, an independent prognostic marker for predicting distant metastasis and survival rates of esophageal squamous cell carcinoma patients. Clin Exp Metastasis 2009;26:1025–32.

— 160 —

CASE REPORT

Rheumatoid arthritis complicated with immunodeficiency-associated lymphoproliferative disorders during treatment with adalimumab

Takahide Ikeda · Syoko Toyama · Michihiro Ogasawara ·
Hirohumi Amano · Yoshinari Takasaki ·
Hiroyuki Morita · Tatsuo Ishizuka

Abstract A 71-year-old woman was diagnosed with rheumatoid arthritis in 2002. Treatment was started with methotrexate and she was switched to adalimumab in 2006. In May 2008, she started complaining of swelling of the left axilla and the left elbow lymph nodes, and adalimumab was discontinued in December. Her lymphadenopathy did not resolve and she was admitted to hospital with fever in May 2009. Subsequent laboratory examinations showed that serum alkaline phosphatase, gamma-glutamyl transpeptidase, C-reactive protein, and soluble interleukin-2 receptor levels were 3,078 IU/l, 510 IU/l, 20 mg/dl, and 7,290 U/ml, respectively. Gallium scintigraphy showed high-intensity areas in the above-mentioned lymph nodes. She suddenly progressed to jaundice and died of pulmonary edema on the 25th day of hospitalization. Autopsy indicated large atypical cells with a distorted nucleus that had multiplied in the above-mentioned lymph nodes. On immunohistochemical staining these cells showed positive staining for CD15, CD30, PAX-5, Epstein-Barr virus (EBV) early small RNA (EBER), and LMP-1. Reactivation of EBV was diagnosed via EBV antibodies and an EBV DNA determination. We considered that she had developed EBV-associated lymphoproliferative disorders due to immunodeficiency caused by adalimumab administration. Reactivation of EBV associated with adalimumab and the relationship of this reactivation to malignant lymphoma have been rarely reported.

Introduction

Rheumatoid arthritis (RA) patients have a high incidence of lymphoma compared with the general population, according to many recent reports. It has been reported that patients receiving methotrexate (MTX), which is one of the mainstays of RA treatment, can develop lymphoproliferative disorders (LPD). Recently, it has been reported that the widespread employment of anti-tumor necrosis factor (TNF)-alpha antibody treatment has resulted in an increased tumor risk brought about by cytokine suppression. According to the World Health Organization *Classification of tumors of haematopoietic and lymphoid tissues* (2008), in the category of immunodeficiency-associated lymphoproliferative disorders there is an item termed 'other iatrogenic immunodeficiency-associated lymphoproliferative disorders' [1]. In regard to this item, it is noted that MTX and antagonists of TNF-alpha may cause LPD. It remains unclear whether RA itself is associated with LPD or whether cytokine-suppressive treatment causes the adverse effect of LPD. We report here a rare case of a patient with RA with Epstein–Barr virus (EBV)-associated LPD caused by immunodeficiency related to adalimumab administration (Figs. 1, 2).

Case report

A 71-year-old woman was diagnosed with RA in 2002. Treatment was started with MTX (8 mg/week), and she was switched to adalimumab (40 mg/2 weeks) in 2006.

T. Ikeda · H. Morita · T. Ishizuka (✉)
Department of General Internal Medicine, Gifu University
Graduate School of Medicine, Yanagido 1-1, Gifu 501-1194,
Japan
e-mail: Ishizuka@gifu-u.ac.jp

S. Toyama · M. Ogasawara · H. Amano · Y. Takasaki
Department of Rheumatology, Juntendo University Graduate
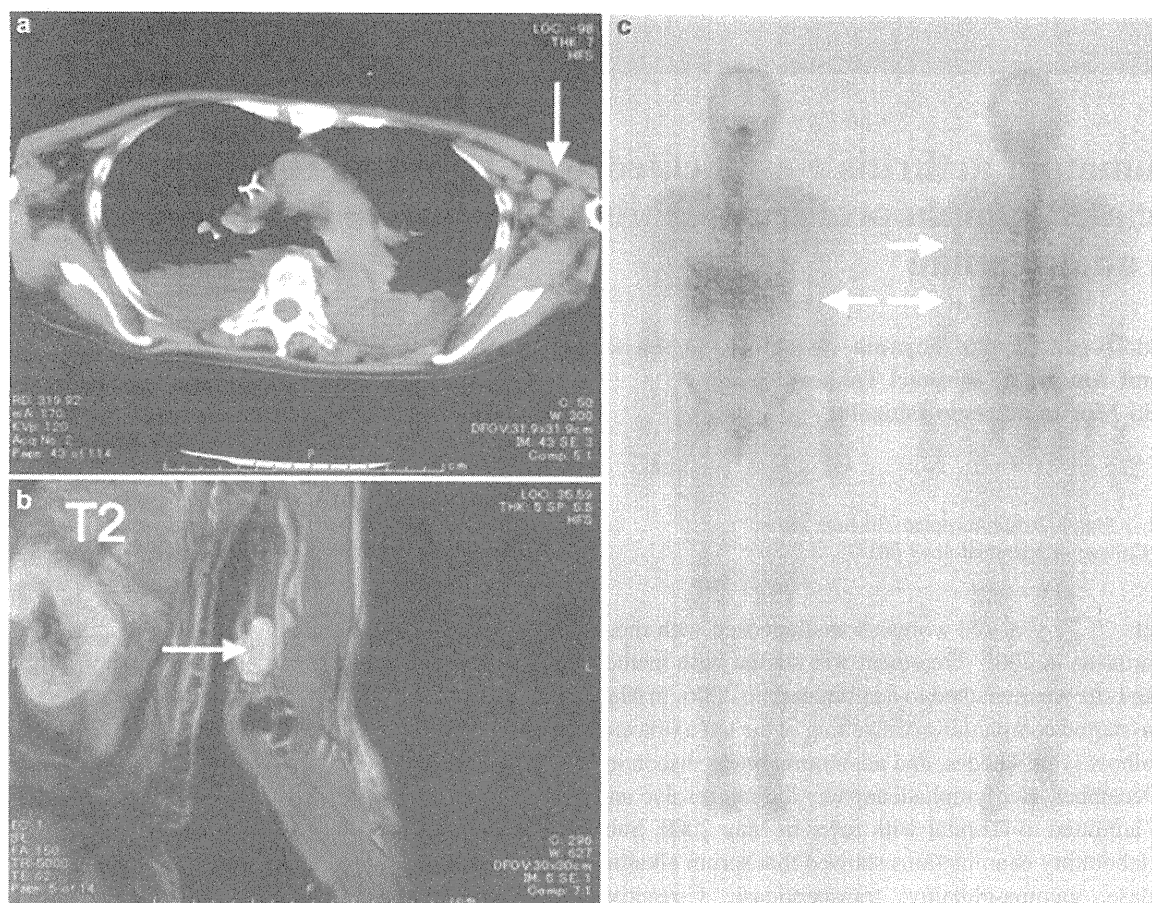School of Medicine, Tokyo 113-8421, Japan

🙂 Springer

Fig. 1 A chest computed tomography (CT) scan showing swollen left axilla lymph nodes (*arrow*; **a**). Magnetic resonance imaging (MRI) showing swollen left elbow lymph nodes (*arrow*; **b**). Gallium scintigraphy showing high-intensity areas in the left axilla and left elbow lymph nodes (*arrows*; **c**)

She complained of swelling of the left axilla and the left elbow lymph nodes starting in May of 2008, and adalimumab was therefore discontinued, in December. Her lymphadenopathy did not resolve. She developed a fever and was admitted to the hospital in May of 2009.

Physical examinations showed swelling of the left axilla and the left elbow lymph nodes without tenderness. The lymph nodes were soft and elastic. She had developed a fever of more than 38°C. She exhibited no arthralgia, joint swelling, or joint distortion.

Laboratory data were as follows: leukocyte count, 4,700/μl (76% neutrophils, 14% lymphocytes, 10% monocytes, 0% eosinophils, and 0.2% basophils); red blood cell count, 3,260,000/μl; hemoglobin, 9.6 g/dl; hematocrit, 29.8%; mean corpuscular volume, 91.4 fl; mean corpuscular hemoglobin concentration, 32.2%; reticulocytes, 1.8%; platelet count, 102,000/μl; serum aspartate aminotransferase, 52 IU/l; alanine aminotransferase, 46 IU/l; lactate dehydrogenase (LDH), 296 IU/l (isozyme LDH1 23%, LDH2 39%, LDH3 22%, and LDH4 7%); alkaline phosphatase (ALP), 3,078 IU/l (isozyme ALP1

19%, ALP2 77%, ALP3 3%, and ALP4 1%); gamma-glutamyl transpeptidase, 510 IU/l; total bilirubin, 2.0 mg/dl; C-reactive protein, 20 mg/dl; ferritin, 6,578 ng/ml; soluble interleukin-2 receptor, 7,290 U/ml; procalcitonin, 0.1 ng/ml; and beta-D glucan, 5.0 pg/ml. Serological tests for antibody titers for EBV were as follows: Anti-VCA IgM antibody, <10 times, anti-VCA IgG, 640 times, anti-EA IgG antibody, 10 times, and anti-EBNA antibody, 20 times. EBV DNA determination in the serum was 6.8×10^3 copies/10^6 cells (normal range; $<2.0 \times 10^1$ copy). A chest and abdominal computed tomography (CT) scan indicated left axilla lymph node swelling and hepatosplenomegaly. Gallium scintigraphy showed high-intensity areas in the left axilla and the left elbow lymph nodes. After we had performed a biopsy of the left axillary lymph node on the 13th day of hospitalization, she suddenly developed jaundice, and she died of pulmonary edema on the 25th day.

After obtaining the consent of the family, we performed an autopsy. The lymph nodes in the left axilla, the left elbow, and the left collarbone fossa, and the paraaortic and hilar lymph nodes had increased in size, up to 4 cm. In
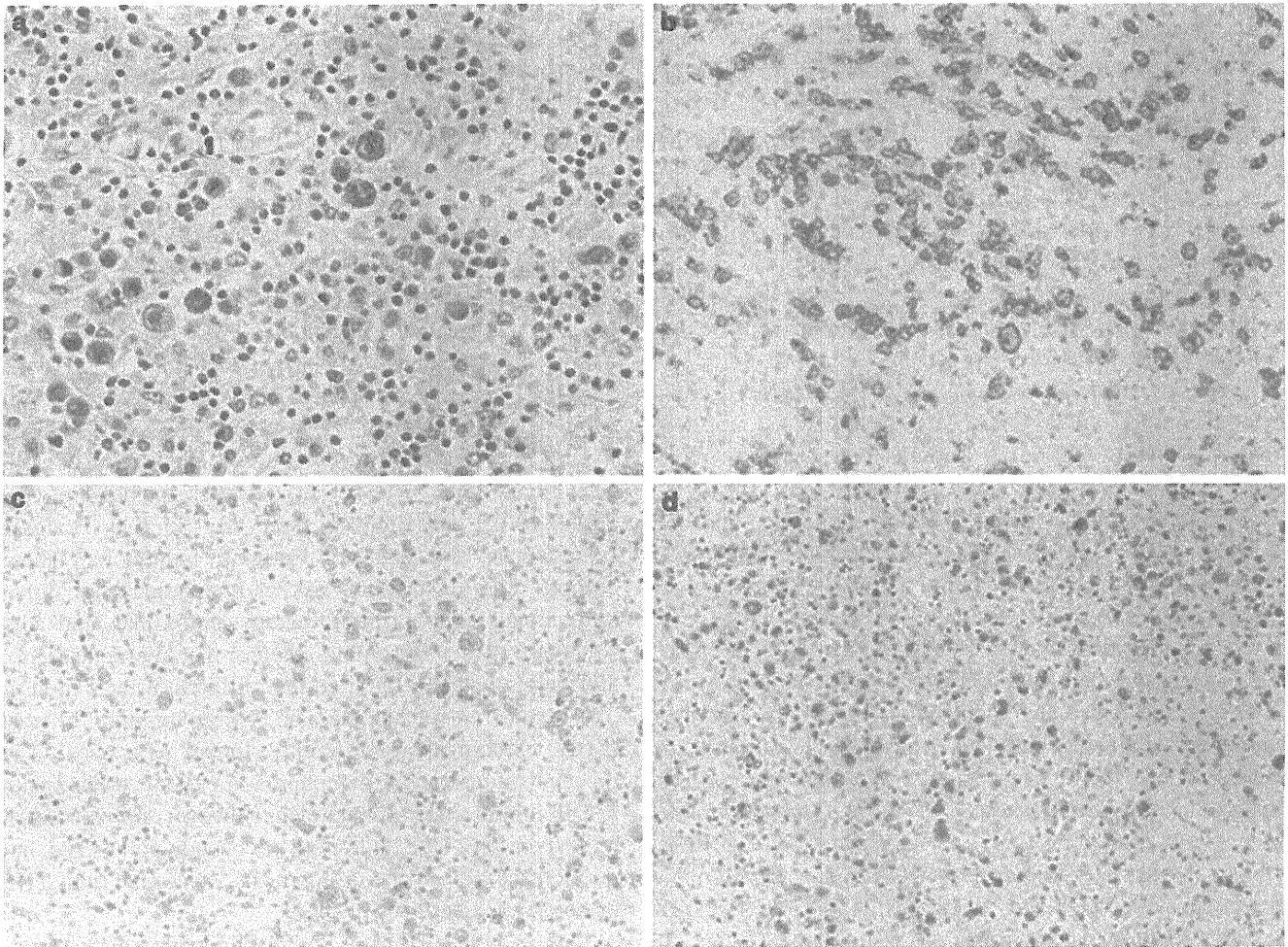
Fig. 2 Lymph nodes showing large atypical cells with distorted nucleus that had multiplied (H&E, ×100) (a). Immunohistochemical staining showing that these cells were positive for CD15 (b), CD30 (c), and Epstein-Barr virus early small RNA (EBER) (d)

these lymph nodes, large atypical cells with a distorted nucleus had multiplied. Immunohistochemical staining of these cells showed positive staining for CD15 (normal granular leukocyte and Hodgkin lymphoma marker), CD30 (Hodgkin lymphoma, anaplastic large T-cell lymphoma, and diffuse large B-cell lymphoma marker), PAX-5 (B-cell marker), EBER (EBV early small RNA), and LMP-1 (EBV encoded latent membrane protein 1). These cells were found to be negative for CD3 (T-cell marker), CD20 (B-cell marker), Oct-2 (B-cell marker), and Bob-1 (B-cell marker). These tumor cells had infiltrated into the liver, spleen, both lungs, the pleura, both adrenal glands, and vertebral marrow, as well as the lymph nodes. Based on the high level of EBV DNA determination, and positive EBER and LMP-1 via immunostaining of the tumor cells, we considered that she had developed EBV-associated lymphoma. Based on the clinical course and pathological results, we made a diagnosis of EBV-associated LPD due to immunodeficiency related to adalimumab administration.

Discussion

It has been reported that patients with RA in Northern Europe have a 1.08–1.4 times increased risk of developing a malignant tumor compared with the general population [2–4], but the majority of reports do not show any significantly increased risk [5–9]. The risk of a malignant lymphoma in patients with RA has been estimated at 1.9–6.7 times that in the general population [3, 4, 7, 9, 10]. Baecklund et al. [11] reported that, in RA patients, the histopathology of malignant lymphoma was B-cell in 78%, with T–natural killer (NK)-cell in 5% and Hodgkin's disease in 6%; 48% of the B-cell malignant lymphomas in RA patients were identified as diffuse large B-cell lymphoma (DLBCL) which is the most common form.

In addition, Baecklund et al. [11] studied the risk of lymphoma in RA patients. They showed that the RA patients with high disease activity and advanced stage had a higher risk of lymphoma compared with controls. In their study, the use of immunosuppressive drugs was kept to a

🖄 Springer

minimum and they found no differences in the characteristics of lymphoma complicated with RA between patients treated with anti-cytokine agents and those treated with other disease-modifying anti rheumatic drugs (DMARDs). Moreover, Wolfe [12] reported that the risk of lymphoma depended on the degree of activity of the RA disease itself, and not on treatment with either MTX or prednisolone. Therefore, it is necessary to consider whether patients with RA with high disease activity have an associated risk of complication with lymphoma. In our case, the patient exhibited no joint distortion or swollen joints, and she did not have high disease activity (stage II, class 1).

There are other reports related to MTX-induced lymphoma complicated with RA. Mariette et al. [13] reported that in 27,000–30,000 RA patients during MTX treatment, the standardized incidence ratio (SIR) of non-Hodgkin's lymphoma was 1.07 (95% confidence interval [CI] 0.6–1.7). Wolfe et al. [10] reported that in 5,500 RA patients during MTX treatment, the SIR of malignant lymphoma was 1.7 (95% CI 0.9–3.2). They could not prove any significant increases of malignant lymphoma in RA patients treated with MTX. However, Kamel et al. [10] reported that many spontaneous malignant lymphomas were attenuated only by stopping MTX treatment. Harris et al. [15] proposed that the above cases of malignant lymphoma should be termed methotrexate-associated lymphoproliferative disorder (MTX–LPD). However, the interrelationship between the duration of treatment with MTX and the onset of LPD [13, 14] still remains unclear. The histopathological characteristics of MTX–LPD appear to be similar to those of DLBCL and Hodgkin lymphoma/Hodgkin-like lymphoma. Of note, EBV was detected in half of the MTX–LPD cases. Therefore, it is suggested that an MTX-induced immunological deficiency state is closely associated with the onset of MTX–LPD.

Recently, the risk of malignant lymphoma in patients treated with biologics has been reported. Askling et al. [16] and Wolfe et al. [17] reported that patients receiving anti-TNF antibody therapy had no significantly increased risk of developing a malignant lymphoma. However, according to the report of Geborek et al. [18], patients receiving anti-TNF antibody therapy had a significantly higher incidence of lymphoma, compared with patients without anti-TNF antibody therapy. According to a meta-analysis of nine large-scale clinical trials associated with RA patients, the risk of developing a malignant tumor was ~3.3 times higher in RA patients than in controls [19]. The use of TNF inhibitors in RA patients should be carefully considered in light of the identification of these agents as risk factors in lymphoma onset. However, the risk of TNF inhibitor-induced onset of malignant lymphoma should be carefully considered because the exacerbation of RA disease activity may itself be a risk factor for the onset of lymphoma. Overseas clinical trials suggest that adalimumab treatment may have caused two cases of EBV reactivation and 23 cases of malignant lymphoma in 12,345 patients with RA, but the associations with EBV still remain unclear. Burmester et al. [20] reported that the SIR of lymphoma in adalimumab-treated patients was 1.09. It was a level similar to that in patients with general articular rheumatism. Miyasaka et al. [21] reported that there was no incidence of malignancy in adalimumab-treated RA patients. Mariette et al. [22] analyzed lymphomas in French RA patients treated with anti-TNF agents from 2004 to 2006; there were 38 cases of lymphoma, 31 non-Hodgkin lymphomas (26 B-cell and five T-cell), five Hodgkin lymphomas, and two Hodgkin-like lymphomas. EBV was detected in both of the Hodgkin-like lymphomas, three of the five Hodgkin lymphomas, and one non-Hodgkin lymphoma. These authors reported that the risk of lymphoma was higher with monoclonal-antibody therapy (infliximab and adalimumab) than with soluble-receptor therapy (etanercept). Horiuchi et al. [23] reported that different effects of anti-TNF agents on transmembrane TNF-alpha might at least partly explain their different clinical efficacies. The mechanism underlying lymphoma in patients treated with a TNF inhibitor is still unknown. However, a direct action of TNF or anti-TNF on B cells has been hypothesized, but no increase in survival or apoptosis was found with TNF or anti-TNF treatment [22, 24].

Our patient exhibited lymphadenopathy during adalimumab treatment 2 years after we had withdrawn MTX treatment. In addition, the disease activity of RA was not so high. Based on the high level of EBV DNA determination and positive EBER via immunostaining of the tumor, we diagnosed this case as reactivation of EBV. Monoclonal integration of EBV in the lymphoma was not studied in our patient, and, although the likelihood of MTX involvement cannot be excluded, the clinical course and pathological results indicated that immunosuppression by adalimumab and the reactivation of EBV had resulted in the development of immunodeficiency-associated LPD. Of note, attenuation of infliximab-related LPD associated with EBV has been reported in an RA patient after treatment with infliximab was stopped [25]. However, in our patient, the lymphoma was exacerbated after adalimumab was stopped. The lymphoma in our patient was associated with EBV reactivation. Therefore, it is suggested that during treatment with a TNF inhibitor and/or MTX, EBV activation should be monitored not only by measuring EBV antibody but also by EBV DNA determination.

Conflict of interest None.

References

1. Swerdlow SH, et al. WHO classification of tumours of haematopoietic and lymphoid tissues. 4th ed. Lyon: IARC; 2008.
2. Kauppi M, et al. Excess risk of lung cancer in patients with rheumatoid arthritis. J Rheumatol. 1996;23(8):1484–5.
3. Mellemkjaer L, et al. Rheumatoid arthritis and cancer risk. Eur J Cancer. 1996;32(10):1753–7.
4. Askling J, et al. Risks of solid cancers in patients with rheumatoid arthritis and after treatment with tumour necrosis factor antagonists. Ann Rheum Dis. 2005;64(10):1421–6.
5. Katusic S. Occurrence of malignant neoplasms in the Rochester, Minnesota, rheumatoid arthritis cohort. Am J Med. Beard CM, Kurland LT, Weis JW, Bergstralh E.1985;78(1A):50–5.
6. Cibere J, et al. Rheumatoid arthritis and the risk of malignancy. Arthritis Rheum. 1997;40(9):1580–6.
7. Thomas E, et al. Risk of malignancy among patients with rheumatic conditions. Int J Cancer. 2000;88(3):497–502.
8. Ekstorm K, et al. Risk of malignant lymphomas in patients with rheumatoid arthritis and in their first degree relatives. Arthritis Rheum. 2003;48(4):963–70.
9. Chiba N. The incidence of cancer among Japanese patients with rheumatoid arthritis in 2003 obtained by using Ninja. Mod Rheumatol. 2006;16(Suppl):202. (abstract).
10. Wolfe F, et al. Lymphoma in rheumatoid arthritis: the effect of methotrexate and anti-tumor necrosis factor therapy in 18,572 patients. Arthritis Rheum. 2004;50:1740–51.
11. Baecklund E, et al. Association of chronic inflammation not its treatment, with increased lymphoma risk in rheumatoid arthritis. Arthritis Rheum. 2006;54:692–701.
12. Wolfe F. Inflammatory activity, but not methotrexate or prednisone use predicts non-Hodgkins lymphoma in rheumatoid arthritis: a 25-year study of 1,767 RA patients. Arthritis Rheum. 1998;41(Suppl 9):188.
13. Mariette X, et al. Lymphomas in rheumatoid arthritis patients treated with methotrexate: a 3-year prospective study in France. Blood. 2002;99(11):3909–15.
14. Kamel OW, et al. Spontaneous regression of lymphoproliferative disorders in patients treated with methotrexate for rheumatoid arthritis and other rheumatic diseases. J Clin Oncol. 1996;14(6):1943–9.
15. Harris NL, et al. World Health Organization classification of tumours. Lyon: IARC Press; 2001. p. 270.
16. Askling J, et al. Haematopoietic malignancies in rheumatoid arthritis: lymphoma risk and characteristics after exposure to tumour necrosis factor antagonists. Ann Rheum Dis. 2005;64: 1414–20.
17. Wolfe F, et al. The effect of methotrexate and anti-tumor necrosis factor therapy on the risk of lymphoma in rheumatoid arthritis in 19,562 patients during 89,710 person-years of observation. Arthritis Rheum. 2007;56:1433–9.
18. Geborek P, et al. Tumour necrosis factor blockers do not increase overall tumour risk in patients with rheumatoid arthritis, but may be associated with an increased risk of lymphomas. Ann Rheum Dis. 2005;64:699–703.
19. Bongartz T, et al. Anti-TNF antibody therapy in rheumatoid arthritis and the risk of serious infections and malignancies. JAMA. 2006;295:2275–85.
20. Burmester GR, et al. Adalimumab alone and in combination with disease-modifying antirheumatic drugs for the treatment of rheumatoid arthritis in clinical practice: the Research in Active Rheumatoid Arthritis (ReAct) trial. Ann Rheum Dis. 2007;66: 732–9.
21. Miyasaka N, The Change Study Investigators, et al. Clinical investigation in highly disease-affected rheumatoid arthritis patients in Japan with adalimumab applying standard and general evaluation: CHANGE study. Mod Rheumatol. 2008;18:252.
22. Mariette X, et al. Lymphoma in patients treated with anti-TNF: results of the 3-year prospective French RATIO registry. Ann Rheum Dis. 2010;69:400–8.
23. Horiuchi T. Transmembrane TNF-alpha: structure, function and interaction with anti-TNF agents. Rheumatology. 2010;49:1215–28.
24. Baran-Marszak F, et al. Effect of tumor necrosis factor alpha and infliximab on apoptosis of B lymphocytes infected or not with Epstein–Barr virus. Cytokine. 2006;33:337–45.
25. Komatsuda A. Reversible infliximab-related lymphoproliferative disorder associated with Epstein–Barr virus in a patient with rheumatoid arthritis. Mod Rheumatol. 2008;18:315–8.

Elevated serum level of circulating syndecan-1 (CD138) in active systemic lupus erythematosus

KENTARO MINOWA, HIROFUMI AMANO, SOUICHIRO NAKANO, SEIICHIRO ANDO, TAKASHI WATANABE, YUTAKA NAKIRI, ERI AMANO, YOSHIAKI TOKANO, SHINJI MORIMOTO, & YOSHINARI TAKASAKI

Department of Internal Medicine and Rheumatology, Juntendo University School of Medicine, Tokyo, Japan

Abstract

Objective: Systemic lupus erythematosus (SLE) is characterized by loss of B cell tolerance and by the presence of polyclonal B cell activation. Syndecan-1 (CD138) is expressed on plasma cells derived from B cells, and is suspected to play a role in SLE. We evaluated the level of soluble CD138 (sCD138) and cell surface expression of CD138 in patients with active SLE, and also examined correlations among the serum levels of BAFF, a proliferation-inducing ligand (APRIL), and CD138 in these patients.

Methods: Peripheral blood samples were obtained from 22 SLE patients in an active disease state and 14 normal controls. The levels of serum sCD138, sBAFF, and sAPRIL were measured using ELISA, and cell surface CD138 was analyzed by flow cytometry. The levels of CD138 mRNA were analyzed by RT-PCR. Blood samples were obtained longitudinally when the patients were in an inactive disease state.

Results: The levels of circulating CD138, CD138 mRNA in PBMC, and the numbers of $CD20^-CD38^+CD138^+$ plasma cells were increased in patients with active SLE in comparison with normal controls. Furthermore, the serum sCD138 level in SLE patients was found to correlate with the proportion of $CD20^-CD38^+CD138^+$ plasma cells. On the other hand, patients with active SLE showed a reduced level of sCD138, and this was inversely correlated with the serum level of sAPRIL.

Conclusions: These results suggest that sCD138 may be applicable as a surrogate marker of disease activity, and that syndecan-1/APRIL signaling may be a potential therapeutic target for patients with active SLE.

Keywords: *Systemic lupus erythematosus, sCD138, plasma cell, BAFF, APRIL*

Introduction

Systemic lupus erythematosus (SLE) is characterized by loss of B cell tolerance and by the presence of polyclonal B cell activation and autoantibody production [1]. Although plasma cells play an important role in the pathogenesis of SLE through production of autoantibody, their function is not well understood. A proliferation-inducing ligand (APRIL), a newly identified member of the tumor necrosis factor (TNF) ligand family, is a type II membrane binding protein of 250 amino acids [2]. APRIL is a close sequence homolog of B-cell-activating factor belonging to the TNF family (BAFF, also known as BLyS), also a member of the TNF family [3].

Originally, APRIL was reported to have a regulatory role in tumor growth. APRIL binds to two of the three BAFF receptors (B cell maturation antigen (BCMA) and transmembrane activator and CAML interactor (TACI)), and is considered to play a regulatory role in B cell proliferation and contributes to plasma cell survival [2,4]. Koyama et al. have detected an elevated serum level of APRIL in patients with SLE, which is correlated slightly with the level of anti-dsDNA antibody (Ab) [5]. Accordingly, APRIL may enhance the longevity of Ab-producing plasma cells in SLE patients.

Syndecan is a member of the integral membrane heparin sulfate (HS) proteoglycan family [6]. Within the bone marrow, syndecan-1 (CD138) is detected solely on the cells of the B lymphocyte lineage, and its expression changes at specific stages of differentiation. Plasma cells, which are terminally differentiated B-lineage cells, are effector cells that produce immunoglobulins involved in the humoral response of adaptive immunity. In mice, syndecan-1 is present on the surface

Correspondence: S. Morimoto, Department of Internal Medicine and Rheumatology, Juntendo University School of Medicine, 2-1-1 Hongo, Bunkyo-ku, Tokyo 113-8421, Japan. Tel: 81358021067. Fax: 81358004893. E-mail: morimoto@juntendo.ac.jp

of pre-B cells, absent in mature B cells, and re-expressed in plasma cells [7]. Previous studies have shown that in patients with myeloma (plasma cell neoplasia), syndecan-1 is shed from the surface of myeloma cells into serum [8]. Also, a recent study has demonstrated very strong binding of APRIL, but not BAFF, to syndecan-1 on the surface of primary multiple myeloma cells [9].

In the present study, on the basis of these findings, we investigated the serum levels of circulating CD138, BAFF, and APRIL levels and analyzed correlation between autoantibody production and these levels in SLE patients.

Materials and methods

Patients and controls

Twenty-two patients with SLE who had been admitted to Juntendo University Hospital in an active disease state were recruited at the first evaluation before treatment for this study. They were subsequently evaluated longitudinally on a second occasion as outpatients when their disease was inactive. As shown in Table I, disease activity in the SLE patients was assessed using the SLE disease activity index (SLEDAI) [10]. Informed consent was obtained from the recruited subjects, and the study was performed in accordance with the principles of the Declaration of Helsinki. The clinical diagnosis in all patients was made in accordance with the 1997 revised criteria of the American College of Rheumatology [11]. Age- and sex-matched volunteers from among the clinical staff were recruited as normal controls. The characteristics of the 22 patients at the time of enrollment are summarized in Table I.

FACS analysis

Fluorescein isothiocyanate-conjugated anti-CD138, phycoerythrin-conjugated anti-CD20, and phycoery-thrin/Cy5-conjugated anti-CD38 were purchased from BD Biosciences (San Jose, CA, USA). Peripheral blood mononuclear cells (PBMCs) were isolated from heparinized venous blood by Ficoll density-gradient centrifugation, and triple-stained with fluorescein isothiocyanate-conjugated anti-CD138, phycoery-thrin-conjugated anti-CD20, and phycoerythrin/Cy5-conjugated anti-CD38. Flow cytometric analysis was performed using FacStation (Becton Dickinson; CA, USA) and the data were processed using the Cell Quest program (Becton Dickinson).

Assay of human sCD138, sBAFF, and sAPRIL

Serum levels of soluble (s) CD138 (syndecan-1), sBAFF, and sAPRIL were determined by sandwich ELISA in accordance with the manufacturer's instructions. The kits used were Syndecan ELISA from Abcam (Cambridge, UK; range 8–256 ng/ml), BAFF ELISA from R&D Systems (Minneapolis, MN, USA; range 62.5–4000 pg/ml), and APRIL ELISA from Bender MedSystems (Vienna, Austria; range 0.78–50 ng/ml).

CD138 mRNA levels in peripheral blood

PBMCs were isolated from heparinized venous blood by Ficoll density-gradient centrifugation, and total RNA was isolated from 1×10^6 PBMCs using an RNeasy Mini kit (QIAGEN, Valencia, CA, USA). RT reactions were undertaken using a High Capacity cDNA Reverse Transcription Kit (Applied BioSystems, Foster City, CA, USA) in accordance with the

Table I.   Cumulative clinical features and clinical manifestations in SLE patients.

Clinical characteristics	SLE ($n = 22$)	
Female: Male	16:6	
Age at the time of study; mean (SD), years	34.4 ± 14.1	
Duration of disease; mean (SD), months	69.7 ± 85.7	
Period until the second evaluation; mean (SD), months	4.5 ± 7.3	
	First, evaluation	Second, evaluation
SLEDAI score; mean (SD) range	10.9 ± 5.9 (5–26)	3.8 ± 1.7 (0–6)
Serological features; mean (SD)		
anti-dsDNA Ab, (IU/ml)	97.8 ± 107.6	24.5 ± 41.9
CH50, (U/ml)	24.2 ± 12.9	32.4 ± 9.1
Medication; mean (n)		
Prednisolone/daily dose, (mg)	21.1 ± 13.5 ($n = 15$)	14.6 ± 10.1 ($n = 21$)
AZA/daily dose, (mg)	None	50 ($n = 3$)
Tacrolimus/daily dose, (mg)	None	2 ($n = 6$)
CYA/daily dose, (mg)	None	75 ($n = 1$)
IVCY, times	None	6 ($n = 1$)

Notes: SLEDAI, Systemic Lupus Erythematosus Disease Activity Index; AZA, Azathioprine; CYA, Cyclosporine; IVCY, Monthly pulse of intravenous cyclophosphamide.

manufacturer's protocol. Quantitative RT-PCR (Q-PCR) was performed as described previously [12]. The sequences of the primers were as follows: CD138 sense: 5'-CTGGGCTGGAATCAGGAATA-3' and anti-sense: 5'-GTGACATTAAGGAGAAGCTGT-GC-3', β-actin sense: 5'-GGAGTTGAAGGTAGTT-TCGTGGA3' and anti-sense: 5'-AGCACTGTGTT-GGCGTACAG-3'.

PCR products were separated on 2% agarose gel and stained with ethidium bromide. Levels of CD138 mRNA were normalized to β-actin for each sample. Statistical analysis was performed using the Mann–Whitney U-test and Pearson's correlation coefficient. Statistical significance was defined as a P-value of <0.05.

Results

Initially, we examined the serum level of sCD138 in patients with SLE and normal controls, and found that it was significantly higher in the former than in the latter ($P < 0.05$; Figure 1a). The serum sCD138 level was also significantly higher in patients with active SLE than in those with inactive disease (Figure 1b). In patients with SLE, the level of PBMC mRNA was significantly increased (Figure 1c,d), and the proportion of $CD20^-CD38^+CD138^+$ plasma cells was higher than that in the normal controls (SLE: 0.13 ± 0.17, NC: 0.04 ± 0.04). Moreover, the population of these cells was increased when SLE was

active (Figure 2a). The serum sCD138 level in SLE patients was correlated with the ratio of $CD20^-CD38^+CD138^+$ plasma cells (Figure 2b).

Next, we investigated the correlation between the serum sCD138 level and disease activity measured in terms of SLEDAI. As shown in Figure 3, there was a significant correlation between these two parameters, the serum sCD138 level being high when disease activity was increased. However, we did not find any significant correlation between the level of sCD138 and other markers of disease activity (anti-dsDNA Ab, C3 and C4; data not shown).

In addition, we examined the correlation among sCD138, sBAFF, and sAPRIL in SLE patients. Although the level of sBAFF in the patients was significantly higher than that in normal controls ($P < 0.05$; Figure 4a), it showed no significant change when the disease was inactive (Figure 4b). The serum sAPRIL level in SLE patients also tended to be higher than that in normal controls (Figure 4c), but was found to be significantly decreased when the disease was active (Figure 4d). When the patients were divided into two groups, high (>50 ng/ml) and low (<50 ng/ml), according to the level of sCD138, patients with a high level of sCD138 had a significantly lower level of sAPRIL than those with a low sCD138 level (Figure 4f). On the other hand, there was no difference in the level of sBAFF between these two groups (Figure 4e).
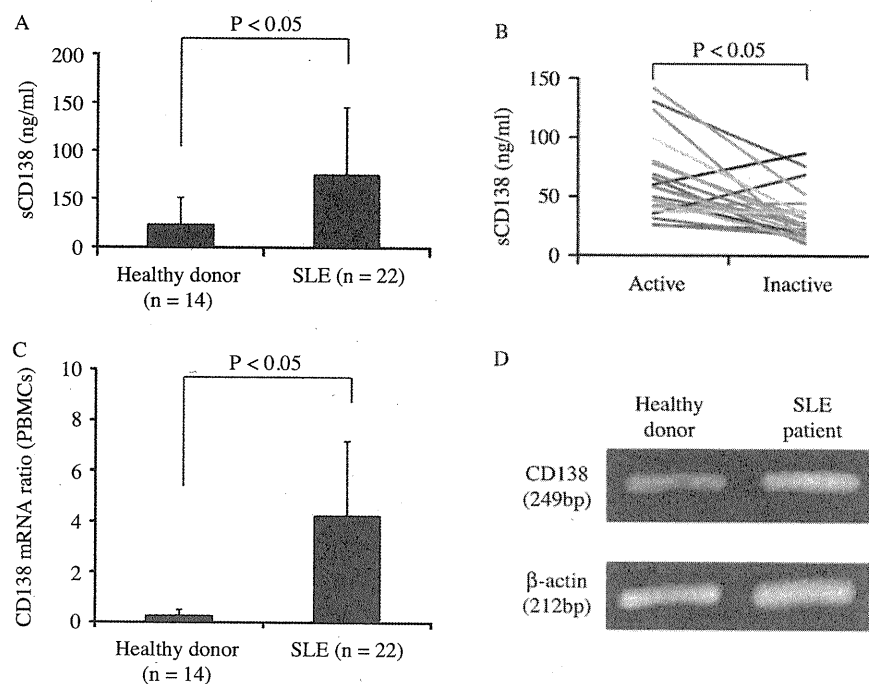

Figure 1. (A) The serum sCD138 level in SLE patients was significantly higher than that in normal controls ($P < 0.05$). (B) Correlation between changes in the serum sCD138 level and changes in the level of disease activity between the first and second evaluations during longitudinal follow-u p of SLE patients. (C) Expression of CD138 mRNA on PBMCs from SLE patients was significantly higher than that in normal controls ($P < 0.05$). (D) CD138 or β-actin samples (10 μl) were used as templates for RT-PCR. The products were separated on 2% Tris-borate-EDTA agarose gels containing 0.5 μg/ml ethidium bromide and visualized under UV. SLE, systemic lupus erythematosus; PBMC, peripheral blood mononuclear cell.
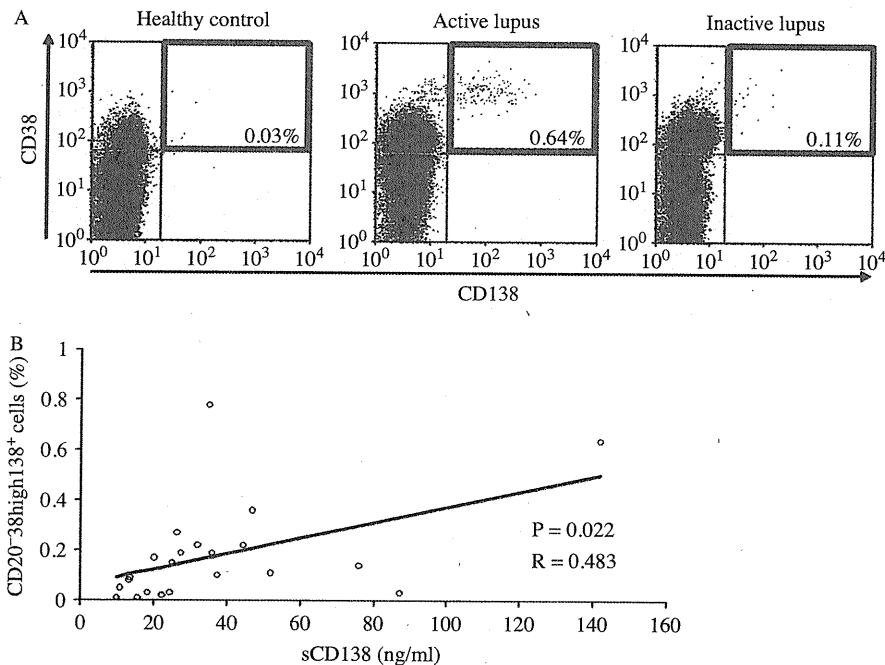
Figure 2.   (A) Surface CD138 expression on CD38⁺ cells among peripheral CD20⁻ cells from patients with active or inactive SLE and healthy controls, examined by flow cytometry. The populations of CD20⁻, CD38 high, and CD138⁺ cells represent plasma cells. (B) A significant correlation was found between sCD138 and CD20⁻, CD38 high, and CD138⁺ plasma cells ($P = 0.022$, $R = 0.483$). SLE, systemic lupus erythematosus.

Discussion

In this study, we showed that the serum level of sCD138 was significantly higher in patients with active SLE than that in patients with inactive disease. Syndecan-1 (CD138), a member of the syndecan family of cell surface transmembrane HS proteoglycans, is expressed on the surface of epithelial cells and plasma cells [6]. Circulating soluble CD138 (sCD138), the intact domain of CD138, is constantly shed from the cell surface [13], and a high level
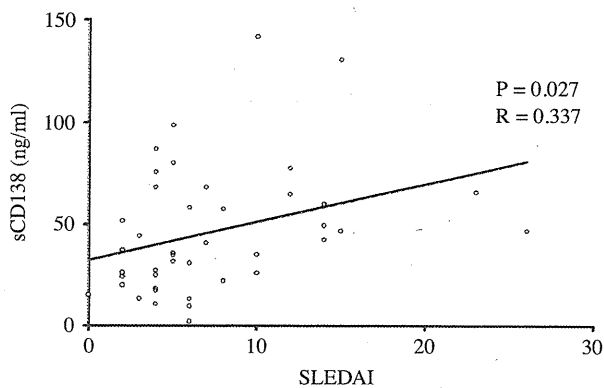

Figure 3.   A significant correlation was found between the serum level of sCD138 and disease activity measured in terms of SLEDAI ($P = 0.027$, $R = 0.337$). SLE, systemic lupus erythematosus; SLEDAI, SLE disease activity index.

of sCD138 has been reported in patients with multiple myeloma [14].

Thus, the presence of sCD138 in serum is the result of expansion and activation of plasma cells. Accordingly, the increased level of sCD138 in serum observed in this study suggested that plasma cells are more activated in patients with active SLE. In fact, we showed that CD138 on the cell surface of PBMCs and the expression of its mRNA were also significantly increased in patients with active SLE, relative to normal controls and patients with inactive disease.

Our study also revealed that, in SLE patients, a high level of serum sCD138 was significantly correlated with increased disease activity and a lower level of serum sAPRIL, whereas it was not correlated with the level of sBAFF. Zhang et al. reported that the serum level of sBAFF was higher in SLE patients than that in normal controls, and was correlated with the titer of anti-dsDNA Ab, although changes in the serum sBAFF level were not correlated with changes in disease activity in individual patients [15].

Stohl et al. also reported that the level of sBAFF was not correlated with changes in disease activity in individual patients [16], and that the serum sAPRIL level showed a significant inverse correlation with serum anti-dsDNA Ab titer and clinical disease activity [17]. Furthermore, Yan et al. reported that APRIL bound mainly to TACI and acted as a negative regulator of B cell activation [18]. In accordance with these reports, our present results revealed that the
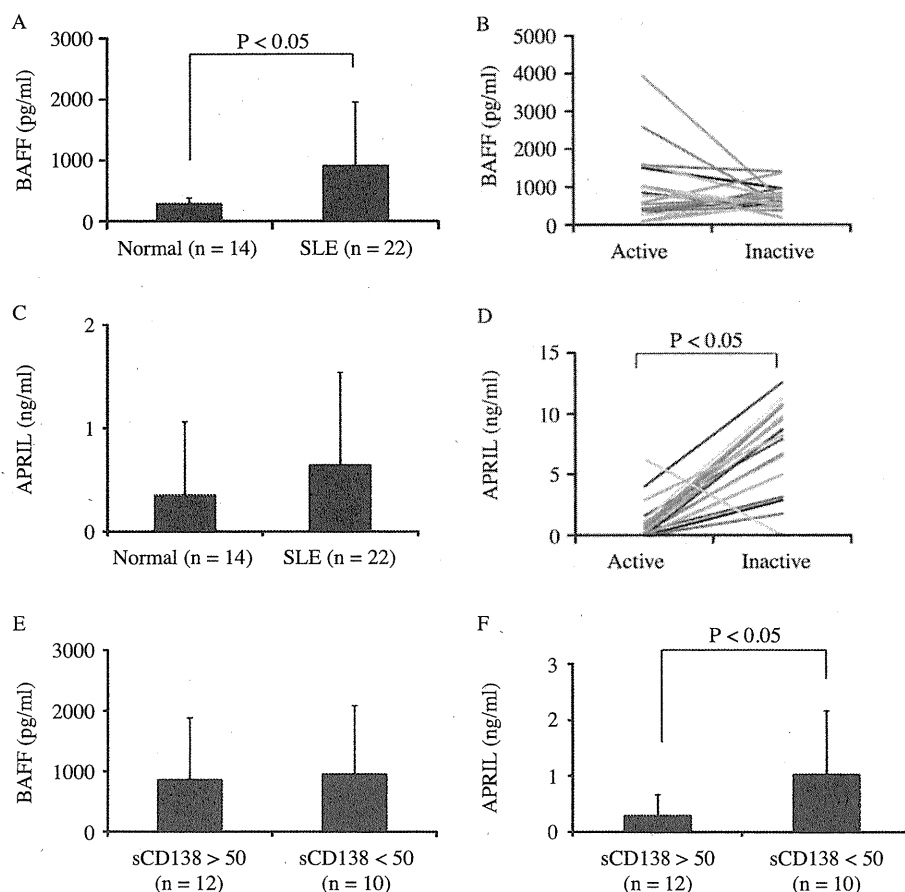
Figure 4. (A) The serum sBAFF level in SLE patients was significantly higher than that in normal controls ($P < 0.05$). (B) Changes in serum sBAFF level in relation to changes in the level of disease activity between the first and second evaluations during longitudinal follow-up of SLE patients. (C) The serum sAPRIL level in SLE patients tended to be higher than that in normal controls. (D) Correlation between changes in the serum level of sBAFF and changes in the disease activity between the first and second evaluations during longitudinal follow-up of SLE patients. (E) Serum sBAFF levels were compared by dividing the patients into two groups on the basis of the sCD138 level: high (>50 ng/ml) and low (<50 ng/ml). (F) Serum sAPRIL levels were compared by dividing the patients into two groups on the basis of the sCD138 level: high (>50 ng/ml) and low (<50 ng/ml). SLE, systemic lupus erythematosus.

serum level of sBAFF was not correlated with SLE disease activity, and that the serum sCD138 level was inversely correlated with the level of sAPRIL.

With regard to the relationship between sCD138 and sAPRIL, syndecan-1 is known to be involved in numerous interactions with extracellular matrix proteins, growth factors, chemokines, and adhesion molecules through HS chains. Recent reports have demonstrated that APRIL can bind to HS chains, and that this binding can be inhibited by heparin [19]. In this scenario, serum sAPRIL is captured by soluble and membrane-bound syndecan-1 HS chains via the lysine-rich region at the *N* terminal portion of APRIL. This would explain why patients with active SLE would have a high level of sCD138 but a significantly lower level of sAPRIL.

Our findings suggest that sCD138 would have potential as a surrogate marker of disease activity, and that syndecan-1 acts as a co-receptor for APRIL, thus promoting activation of the APRIL/TACI and/or

BCMA pathway responsible for the production of autoantibody. Accordingly, the syndecan-1/APRIL signaling pathway could be a potential therapeutic target for patients with active SLE.

Acknowledgements

Declaration of interest: The authors report no conflicts of interest. The authors alone are responsible for the content and writing of the paper.

References

[1] Grammer AC, Lipsky PE. B cell abnormalities in systemic lupus erythematosus. Arthritis Res Ther 2003;5(Suppl 4): S22–S27.

[2] Hahne M, Kataoka T, Schroter M, Hofmann K, Irmler M, Bodmer JL, Schneider P, Bornand T, Holler N, French LE, Sordat B, Rimoldi D, Tschopp J. APRIL, a new ligand of the tumor necrosis factor family, stimulates tumor cell growth. J Exp Med 1998;188:1185–1190.

[3] Koyama T, Tsukamoto H, Masumoto K, Himeji D, Hayashi K, Harada M, Horiuchi T. A novel polymorphism of the human APRIL gene is associated with systemic lupus erythematosus. Rheumatology (Oxford) 2003;42:980–985.

[4] Belnoue E, Pihlgren M, McGaha TL, Tougne C, Rochat AF, Bossen C, Schneider P, Huard B, Lambert PH, Siegrist CA. APRIL is critical for plasmablast survival in the bone marrow and poorly expressed by early-life bone marrow stromal cells. Blood 2008;111:2755–2764.

[5] Koyama T, Tsukamoto H, Miyagi Y, Himeji D, Otsuka J, Miyagawa H, Harada M, Horiuchi T. Raised serum APRIL levels in patients with systemic lupus erythematosus. Ann Rheum Dis 2005;64:1065–1067.

[6] Carey DJ. Syndecans: Multifunctional cell-surface co-receptors. Biochem J 1997;327:1–16.

[7] Sanderson RD, Lalor P, Bernfield M. B lymphocytes express and lose syndecan at specific stages of differentiation. Cell Regul 1989;1:27–35.

[8] Dhodapkar MV, Kelly T, Theus A, Athota AB, Barlogie B, Sanderson RD. Elevated levels of shed syndecan-1 correlate with tumour mass and decreased matrix metalloproteinase-9 activity in the serum of patients with multiple myeloma. Br J Haematol 1997;99:368–371.

[9] Moreaux J, Sprynski AC, Dillon SR, Mahtouk K, Jourdan M, Ythier A, Moine P, Robert N, Jourdan E, Rossi JF, Klein B. APRIL and TACI interact with syndecan-1 on the surface of multiple myeloma cells to form an essential survival loop. Eur J Haematol 2009;83:119–129.

[10] Bombardier C, Gladman DD, Urowitz MB, Caron D, Chang CH. Derivation of the SLEDAI: A disease activity index for lupus patients. The Committee on Prognosis Studies in SLE. Arthritis Rheum 1992;35:630–640.

[11] Hochberg MC. Updating the American College of Rheumatology revised criteria for the classification of systemic lupus erythematosus. Arthritis Rheum 1997;40:1725.

[12] Nakano S, Morimoto S, Suzuki S, Watanabe T, Amano H, Takasaki Y. Up-regulation of the endoplasmic reticulum transmembrane protein UNC93B in the B cells of patients with active systemic lupus erythematosus. Rheumatology (Oxford) 2010;49:876–881.

[13] Fitzgerald ML, Wang Z, Park PW, Murphy G, Bernfield M. Shedding of syndecan-1 and -4 ectodomains is regulated by multiple signaling pathways and mediated by a TIMP-3-sensitive metalloproteinase. J Cell Biol 2000;148:811–824.

[14] Seidel C, Sundan A, Hjorth M, Turesson I, Dahl IM, Abildgaard N, Waage A, Borset M. Serum syndecan-1: A new independent prognostic marker in multiple myeloma. Blood 2000;95:388–392.

[15] Zhang J, Roschke V, Baker KP, Wang Z, Alarcon GS, Fessler BJ, Bastian H, Kimberly RP, Zhou T. Cutting edge: A role for B lymphocyte stimulator in systemic lupus erythematosus. J Immunol 2001;166:6–10.

[16] Stohl W, Metyas S, Tan SM, Cheema GS, Oamar B, Xu D, Roschke V, Wu Y, Baker KP, Hilbert DM. B lymphocyte stimulator overexpression in patients with systemic lupus erythematosus: Longitudinal observations. Arthritis Rheum 2003;48:3475–3486.

[17] Stohl W, Metyas S, Tan SM, Cheema GS, Oamar B, Roschke V, Wu Y, Baker KP, Hilbert DM. Inverse association between circulating APRIL levels and serological and clinical disease activity in patients with systemic lupus erythematosus. Ann Rheum Dis 2004;63:1096–1103.

[18] Yan M, Wang H, Chan B, Roose-Girma M, Erickson S, Baker T, Tumas D, Grewal IS, Dixit VM. Activation and accumulation of B cells in TACI-deficient mice. Nat Immunol 2001;2:638–643.

[19] Alexopoulou AN, Multhaupt HA, Couchman JR. Syndecans in wound healing, inflammation and vascular biology. Int J Biochem Cell Biol 2007;39:505–528.